

Critical Interfacial Bonding Strength Improvements for Surface Modifications Through Electro-Plasma-Processing (EPP) and Biomimetic

Naser I. Hossain, Muhammad A. Wahab¹, Jiandong Liang

Department of Mechanical & Industrial Engineering, Louisiana State University and A. & M. College,
Central Campus, 3261-Patrick F. Taylor Hall, Engineering Lane,
Baton Rouge, Louisiana, LA 70803, USA.

Abstract- Protections of expensive alloy elements within the surface coatings from high temperature and corrosive environments have always been an engineering challenge when the high maintenance, repair cost, and failures from thermal stresses are considered. This study deals primarily with the finite element simulation of these inter-locking mechanisms for surface modifications. The interlocking geometries are formulated in an electro-mechanical process known as *Electrolytic-Plasma-Processing* (EPP) that generates an array of unique micro-geometries on material surfaces. To simulate the mechanical and thermal loads on the different micro-geometries, the commercial finite element software was used along with SolidWorks for array modelling. The salient characteristic of this research is the analogy that was drawn between biological, *Van Der Waals* dry adhesion mechanism in Gecko feet, and that of the superficial surface of the “*Thermally Grown Oxide* (TGO)” layer in Thermal-Barrier-Coatings—(TBC). Since the micro-geometry, resembling “mushroom-heads” in the Gecko feet provided improved adhesion up to, as much as 10-folds, compared to other geometries (i.e., spatula head, spherical head, or plain triangular crevices) analyzed. The findings of this study can attribute to the following: (i). EPP-treatment effectively modifies the surface of metals and alloys to be coated and produces an expedient morphological change that increases adhesion. (ii). The EPP-surface features have a longer shelf-life than many of its comparable technologies, making it even more economically attractive; and which applies, especially during corrosion applications. (iii). The “mushroom-head” geometry has been classically proven to be an aide to bio-adhesion; and this work further strengthens the argument and encourages new research in this direction.

Keywords- *Electro-Plasma-Processing* (EPP); *surface modifications*, *mushroom-head geometry*; *Van Der Waals force*; *dry adhesion mechanism*; *thermal- barrier- coatings* (TBC); *finite element analysis* (FEA).

I. INTRODUCTION

There have been tremendous interest to find answers for many complex engineering problems from Mother Nature; but up until now, there are limited investigations reported in the Open literature about the mysterious resemblance between *Mother Nature* and the manufactured scientific phenomenon in the fields of adhesion and thermal protection. Adhesion, despite being a common phenomenon in nature was incredibly hard to characterize or control in the use of industrial applications. Engineers have struggled to

find an optimal and economic way of bonding protective coatings onto expensive base metals without somehow changing the chemical nature of the base metal itself. Chemical bonding processes often introduce fragility and fracture-weakness to the crystal structure of the base metal/alloy, sometimes even attributing to corrosion-based metal depletions. To relate and apply natural laws and designs to something synthetic, like industrial coating adhesion, a systematic mathematical study supported by proven hypothesis- literature and numeric models are needed. The underlying effort that has been generated by the mechanical properties of contact surfaces is the surprising range of surface mechanical properties such as adhesion, friction, and compliance that are mostly attained by the design of near-surface architecture using generic material properties [1, 2]; which is a new scope in adhesion mechanics. It has been reported by this research group as well as others that *Electrolytic-Plasma-Processing* (EPP) is an efficient surface modification method for metallic materials; and Liang et al., [3], reported a novel work on the electro-plasma-processing earlier. With proper control of the process parameters, EPP could generate unique surface morphology, which is suitable for effective surface coatings and cleaning of the metallic surfaces and surface modifications; inherently, good adhesion strength can be achieved for eventual coating the surfaces or substrates. The motivations behind this study are: (i) to provide an increased understanding in both qualitative and a quantitative summation from the engineering point of view on the issues of adhesion, friction, repulsion, and compliance in thermal barrier coating systems; and (ii) how bio-mimicry or adaptations from the *Mother Nature* can be harnessed to give an acceptable solution to a complex problem facing the field of industrial thermal protection.

II. PHENOMENOLOGY AND RESEMBLANCE

This research has put forward a novel challenges and contemplates on the similarities between adhesion in metal surfaces and adhesion in biological substances; and accordingly, a numerically validated model has been generated. The phenomenon observed in this process is therefore, comparable to both synthetic fabrication and natural synthesis in the animal and insect world. Results obtained from the study shows clearly the concepts from

biological examples that can be transferred to realistic engineering problems with carefully designed experiments.

II.A. Concepts of Adaptation in Engineering Applications

The emerging field of *biomimetic* is already gaining a foothold in the scientific and technical fields. Over billions of years of evolution, *Nature* has utilized basic materials to provide a breathtaking array of functionality to its creations, and we are discovering that possible means for doing this, is the clever use of hierarchical structures. As we understand the underlying mechanisms [1-5], we can begin to harness them for commercial applications. Significant advancements in nanofabrication have allowed engineers to replicate structures of interest in biomimetic using smart materials and shape memory alloys. The commercial applications include nanomaterials, nano-devices, and processes that may even enable self-cleaning surfaces, etc. Some of these applications may, at first, seem magical or even unrealistic, but they are simply the results of applying science and engineering to the uncovering of the secrets of the Nature.

A nanostructured-engineered material based on Gecko-feet reusable adhesive would have a wide range of applications, from everyday objects such as, adhesive tapes and fasteners to exotic items namely, wall-climbing robots. However, for engineering applications such material is not quite so straightforward. The design has to ensure that the fibrils are compliant enough to easily deform when pressed against a rough surface, but remain rigid enough not to collapse/buckle under their own weight. Spacing between the individual fibrils is also important: i.e., for too small size

and adjacent fibrils can attract each other through intermolecular forces, which will lead to bunching/clustering. As Ji *et al.* [6]-described the limits of current fabrication methods must also be taken into considerations.

II.B. Preparation of Target Materials and Plasma Bombardment

The commercial AISI-1018 low carbon steel was used in this study (wt% 0.18 C, 0.6 Mn, <0.05 S, and Fe-balance) for Electrolytic-Plasma-Processing [7, 8]. Samples were first mirror polished with SiC paper to a grit level of 2400; then ultrasonic cleaning was conducted in ethanol for improving the surface finish. Scanning Electron Microscopy (SEM) and Energy-Dispersive X-ray Spectroscopy (EDAX) were performed on the sample surfaces. The mirror-polished samples were then subjected to EPP- treatment at 150 V for 5 minutes and 15 minutes, respectively.

The EPP- cell has similar components of electrochemical cell as shown in Fig. 2.1. The CGD (Contact Glow Discharge) configuration was adopted; hence, the electrical circuit remains the same except that the bath solution was enclosed in a chamber, which could be sealed and pressurized (Fig. 2.2 (c)). Argon was used to pressurize the chamber, since pressurized argon could dilute the hydrogen and oxygen generated from electrochemical reactions for safety purpose. Figures 2.2 (a) and (d) represent the electrodes and assembly of the electrodes, respectively. The power density on the metal top surface is few orders of magnitude higher than conventional electrochemical treatments. This was sufficient to generate an envelope of plasma bubbles around the electrode materials.

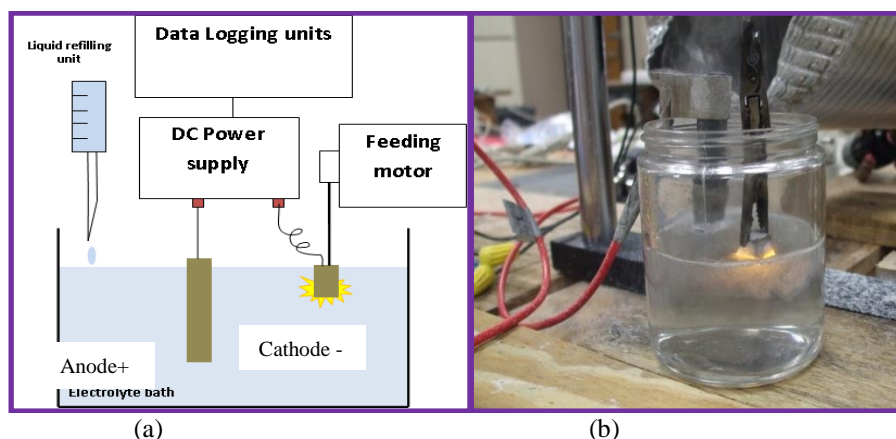


Fig. 2.1: (a) Electrolytic-Plasma-Process (EPP) configuration; (b) Photo of EPP for Contact Glow Discharge (CGD) electrolysis [8]

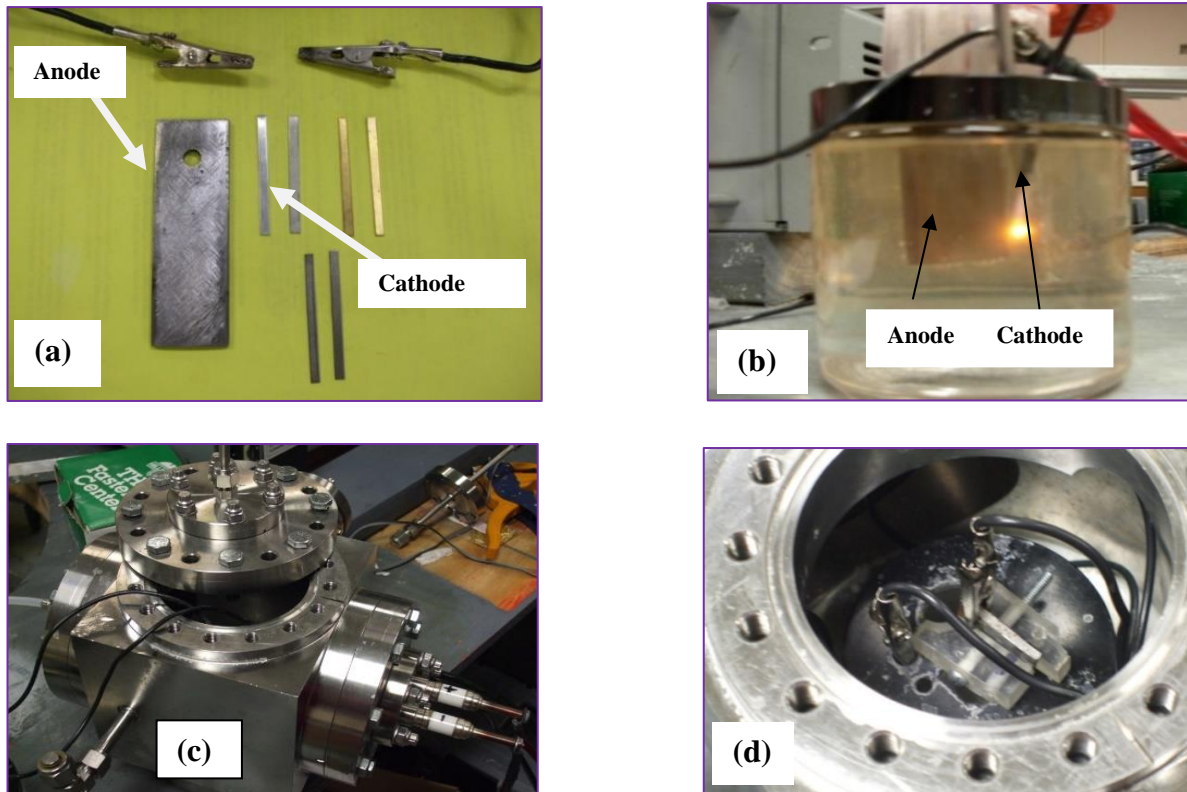


Fig. 2.2: (a) Electrolysis electrodes; (b) Contact glow discharge and plasma bubble envelop during EPP- run on target material, (c) Process Chamber Assembly, (d) pressure chamber with Electrodes. [8]

Distilled water was supplied with a refilling device in order to compensate the vaporization of water and hence the electrolyte concentration was maintained. The electrolyte used was Na_2CO_3 solution with concentration of 75g/L, and equivalent electrical conductivity of 43.1 ± 0.5 mS/cm. The voltage supply was fixed at 150 V and the target surface was connected as a cathode with the power supply unit. The plasma discharge and operation included following four separate stages:

- (i). The introductory reduction reaction on the target electrode/material and the formation of violent, nebular bubbles;
- (ii). There is a strong but steady increase of electric current, near surface electrolyte experiences transition from one intermediate plasma state to another, and boiling initiates due to intense joule-heating;
- (iii). Quasi-stable film forms near the target material surface and apparent current drop is observed [7, 8, 9]; and
- (iv). Increasing the voltage further, leads to a noticeably stable and luminous plasma discharge on metal surface.

These stages mentioned above develop due to change in the current. Depending on the additional operational parameters, the current density could reach up to 10 A/cm^2 . The surface plasma also develops high temperature ($>2000^\circ\text{C}$) and short life (microseconds) and small affected area (nm to μm radius). The surface metal is partially melted by the intense heat. The cold liquid immediately quenches the molten metal as the plasma locally collapses after each discharge and quenches the metal. The micro explosions caused by the plasma bubbles leads to a unique metamorphic shape on the surface. Furthermore, such repetitive rapid heating and quenching impingement generates refined microstructures on target metal surface. These microstructures under further observation closely resemble “mushroom-head” geometry akin to that found on Gecko and insect feet [Fig. 2.3].

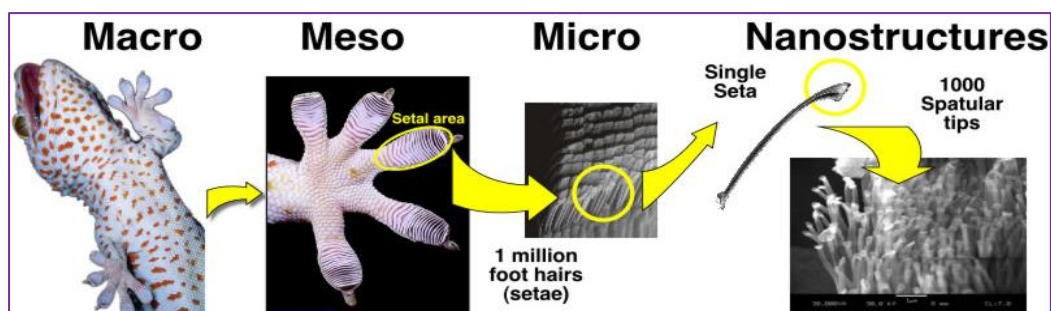


Fig. 2.3: Hierarchical arrangement of microstructure under Gecko feet, at different levels [9, 10]

This is because the hierarchy and array-like distribution displayed underneath the biologically fragmented Gecko feet are similar to the permanent array of protrusions on EPP- treated surfaces. Thus, this electrochemical process reasonably mimics the creations of microstructures in Gecko feet both geometrically and pattern-wise.

II.C. Bio-Adhesion and its Salient Features

Bio-adhesion can be described as a phenomenon observed in nature where the hierarchical, micro/nano scale geometries in the legs or pods of animals and insects assist adhesion to rough surfaces through dry adhesion [10, 11]; and closely approximate *Van Der Waals* attraction forces [6, 9]. This is an ingenious way of achieving adhesion as this does not need a secretory gland constantly producing adhesive for achieving wet-adhesion, thus simplifying the actual “stiction process”. Studies have shown that this extraordinary adhesive capability (almost, 28 mN/fibril [11]) can be separated into two parts: (i) an adaptation of a hierarchical structure of the pods to a natural, rough surface, and (ii) the mechanics of adhesion of a single contact with surfaces.

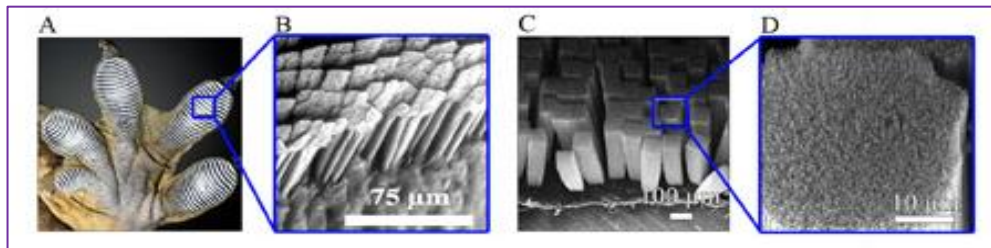


Fig. 2.4: Hierarchical micro/meso level structures that attribute to the interatomic ‘Van Der Waals’ adhesion in Gecko feet [12]

Figure 2.4 above shows the hierarchical structure containing a series of regular arrangements, almost identically orientated lamellae. General electronic microscopy has shown that the lamella is composed of uniform hair-like fibers (setae) which branch-out at the tips into finer fibrillae (spatulae). These structures allow for intimate contact between the spatulae and surfaces to obtain high adhesion via the ‘van der Waals’ force [1] on almost any surfaces. The adhesive force of single Gecko setae was measured by Autumn et al. [4]. Their experimental results showed that single setae could make maximum adhesive force of nearly 20-µN and maximum shear adhesive force equivalent of 200 µN. This means that a contact area of 1.0 cm² could produce a normal adhesive force of 10 N and a shear adhesive force of 100 N, based on a Tokay Gecko (Gekko, gekko) pedal parameters, which has about 5000 setae per mm² as also shown in the works of Ji et al. [6].

Zhang and Wen measured an adhesive force of about 10 nN of a single Gecko spatula [12]. In fact, examples from the nature have revealed that many bio systems including insects and geckoes have utilized the nano-scale adhesive contact quite well by the fibril tip on their bio-pads as described by Chan et al. [13]. They discovered contact splitting (a division of a contact area into a number of finer contact elements) and different nano-scale tip shapes of fibril on their pads to enhance separation strength or adhesive efficiency. The principle of contact splitting has been demonstrated by an optimization of fibrillar density as observed in a variety of insects (beetles, flies, and spiders) and Geckos. Larger animals have higher density of fibrils since pull-off strength increases as fibril radius decrease [14].

Kim et al. [15] have extensively studied the adhesion of solid elastic bodies (Fig. 2.5); meanwhile, Weiss discussed various other aspects of adhesion mechanisms and their quantitative assessment in surface coatings conditions [16].

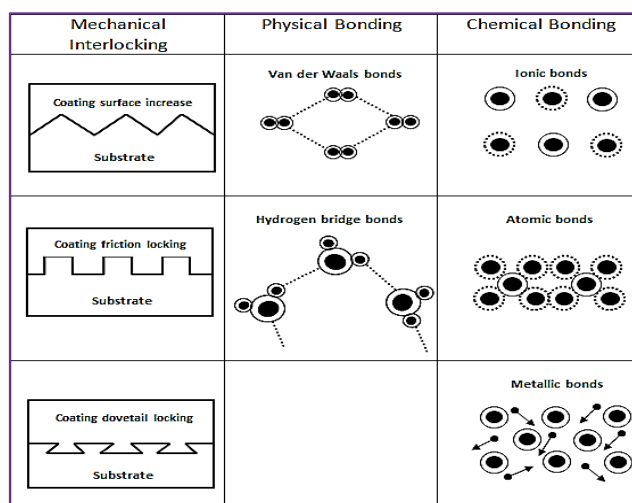


Fig. 2.5: Schematic diagram of the different bonding mechanism [15]

Two general models of the contact behavior have been proposed: (i) the Derjagin-Muller-Toporov (DMT) approach for small, stiff, and low surface energy systems; and (ii) the Johnson-Kendall-Roberts (JKR) [17] theory for large, soft, and high surface energy systems.

The DMT model for 'sphere-on-flat' contact predicts that the local contact stress transforms from compression to tension at the edge of contact area and attractive forces arise in the zone of molecular separation, just outside the contact area. In the JKR model, on the other hand, the attractive forces are assumed to act inside the contact area, and tensile stresses are again exerted close to the contact edge.

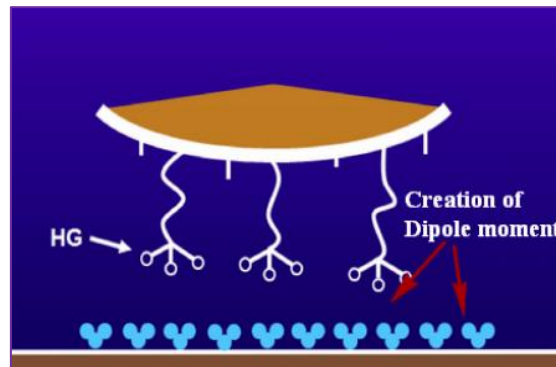


Fig. 2.6: Creation of dipole moments in the micro scale

Thus, it might be expected that adhesion be rather correlated with the contact perimeter than the contact area. A consequence of splitting up a large contact into finer sub-contacts or, alternatively, subtracting finer sub-areas from this large contact, causes increasing the contact perimeter, which should increase adhesion. The creation of the dipole moment, which causes the adhesion (Fig. 2.6) in biological membranes, can also be mimicked for metal surfaces, which is the very essence of this research.

III. WORKFLOW AND METHODOLOGY

This study to substantiate the relation between biological adhesion and commercial grade adhesion in thermal-barrier-coating systems can be divided into several elementary steps. First, the method started by developing an experimental methodology supported by mathematical formulation; next, numerical analysis was performed and validation of model was carried out; and finally, the results and analysis of the synergistic outputs were given.

III.A. Experimental Details

The EPP has already been established as an advanced surface modification technology [10, 14, 18 - 22] whereas; plasma bubbles are being used to bring unique morphological changes to the surface of metals and alloys. Based on Gupta et al. [9] works, our group conducted an extensive experiential program [7, 8, 19, and 22] to understand the surface morphology of the EPP-treated surfaces, and the selected surface features of oxidized and EPP- treated samples are shown in Fig 3.1. Fig 3.1(a) shows the oxidized surfaces on SS304 surface when subjected to 1- hour oxidation at 800°C. With increase of time, larger oxides form and agglomerate. Exfoliation occurs due to expansion during cooling and leads many cracks and blocks of oxides in the final images. EPP- cleaned surface morphologies are shown in Fig. 3.1(b). Special patterns of cleaned surface are due to the melting and rapid quenching of top materials during plasma discharge. The size of micro fingers and spheroids depends on the initial surface feature. With 1.0 hr. oxidation, the surface oxides are much smaller (100-500 nm) than the characteristic structure size of the block (2 – 5µm) on the 50hr. and 100hr. oxidized surfaces. Hence, the EPP- treated feature has large size on 50 hr. and 100 hr. samples and gives mushroom-head shapes which has been considered in the numerical simulation experimentations.

A comparative study of the chemical yields of anodic and cathodic Contact Glow Discharge Electrolysis (CGDE) indicates that the breakup of water molecules occurs entirely in the plasma during cathodic CGDE, but primarily in the liquid (electrolyzed water) and partly in the plasma during the anodic phenomenon. The superficial plasma accumulation and the subsequent explosive collapse of the plasma bubbles in contact with the semi-melted metal/allow surface creates the unique geometry that was studied for its role in adhesion improvement (Fig. 3.2). As seen in Fig. 3.2 the plasma explosions generate a unique morphology on the metal surface.

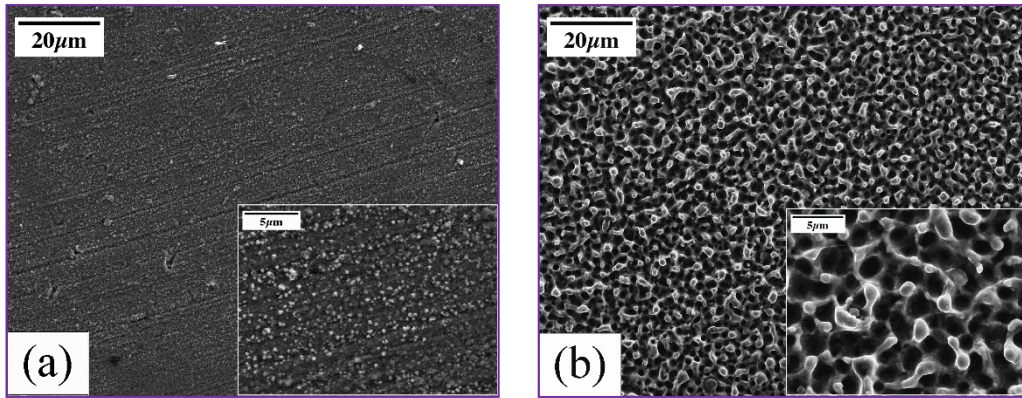


Fig. 3.1: (a) Micro roughness profile of oxidized surfaces; (b) SEM micrograph of a typical EPP- cleaned surface morphology [8, 19]

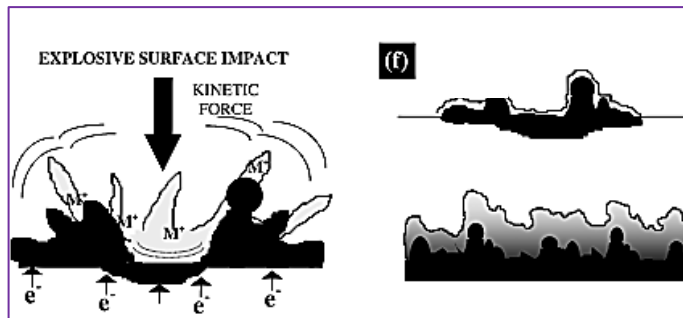


Fig. 3.2: Schematic of the final phase of EPP and generation of desired morphology [11].

III.B. Mathematics of Shape-Effect in Adhesive Contact

Most theories in classical contact mechanics, including DMT, JKR, and Maugis–Dugdale (MD) [9] models concentrate on contact between parabolic surfaces with a curvature expression of $r^2/2R$, where r -is the radius of curvature and R is the characteristic length. In this case, the ‘pull-off’ force ranges between $3\pi R\Delta\gamma/2$ and $2\pi R\Delta\gamma$ depending on the Tabor number of the problem under consideration [9].

On the other hand, the pull-off force is strongly influenced by the surface contour of the contact bodies. To show this point, a simple formula was mentioned by Yao & Gao [18] for a frictionless axisymmetric rigid punch having an arbitrary profile $z = f(r/a)$ in contact with an elastic half-space (not axisymmetric). In this case, the stress distribution (tension being positive) underneath the punch is given by:

$$\sigma_{zz}(r, 0) = -\frac{E^*}{2a} \left[\frac{\chi(1)}{\sqrt{1-r^2/a^2}} - \int_{r/a}^1 \frac{\chi'(t)}{\sqrt{t^2-r^2/a^2}} dt \right] \quad (1)$$

Where,

$$\chi(t) = \frac{2}{\pi} \left[\delta - t \int_0^t \frac{f'(x)}{\sqrt{t^2-x^2}} dx \right], \quad E^* = \frac{E}{1-\nu^2} \quad (2)$$

Equations-1 and 2 are the two major mathematical formulation used to model the contact mechanics in the commercial finite element software COMSOL, using COMSOL’s custom boundary equation input window as well as the finite difference MUMPS solver input dialogue.

Theoretically, when two adjacent atoms approach in a distance of nanometer or less, various interatomic potentials have been proposed to describe the interaction. Among them, the *Lennard-Jones potential* is one of the widely used functions because of its simplicity and inverse sixth-power attractive van der Waals term, which is shown below:

$$\omega(r) = 4\epsilon \left[\left(\frac{\sigma}{r} \right)^{12} - \left(\frac{\sigma}{r} \right)^6 \right] \quad (3)$$

Where, ε is a parameter determining the depth of the potential well [8] and σ is a length scale parameter determining the minimum position of the potential. Then by triple integration of the Lennard-Jones potential, the interaction force between two surfaces can be given by the following equation:

$$p(h) = \frac{8\Delta\gamma}{3e} \left[\left(\frac{e}{h} \right)^9 - \left(\frac{e}{h} \right)^3 \right] \quad (4)$$

Where, p is the pressure exerted by one surface on the other, h is the vertical separation between the corresponding point pairs on the two interacting surfaces, $\Delta\gamma$ is the work of adhesion, or surface-free energy and e is the local equilibrium separation.

III.C. Contour Detection and Coordinate Mapping

MATLAB algorithm was used to digitally map the contours of the shapes appearing on EPP-treated surfaces. The algorithm used was imported for further implementation using the API export environment of an open source image processing workflow called “CellTracer” developed by the research group of Wang [23]. The MATLAB code uses a built in image processing toolbox and a technique called “image segmentation” to map the contour of any geometry from a raster image to an accuracy of $1 \times 10^{-3} \mu\text{m}$. In this case, the images were snapshots of SEM micrographs were taken from the EPP- runs on different surfaces. The evaluation was done to find out an average aspect ratio (height, radius, and curvature) of the common geometric pattern appearing in EPP- treated surfaces. The images were then overlaid and their contour traced with the MATLAB code.

This dimensional measurement and coordinate data was later used to model the array of micro geometries in CAD software (SolidWorks) and analyze their adhesion strength numerically in a FE interface.

Figure 3.3 shows the different steps of the contour mapping process using MATLAB’s image processing toolbox in the absence of a profilometer. The image acquisition was done with open source, “fractal image capture software” called “Fast Stone Capture”. The scales of measurement measuring up to around $15 \mu\text{m}$ were taken from the SEM micrograph inspection software as shown in Figure 3.1(a). The inversion, sharpening, feature detection, and overlaying as well as coordinate tracking were done with CellTracer Matlab Code. The data points acquired were averaged with an integral averaging algorithm. When combined with the works of Del Campo [10] on other tip-shapes and micro geometries, Table-1 can be formed for the comparison of the size effect in adhesion process [11].

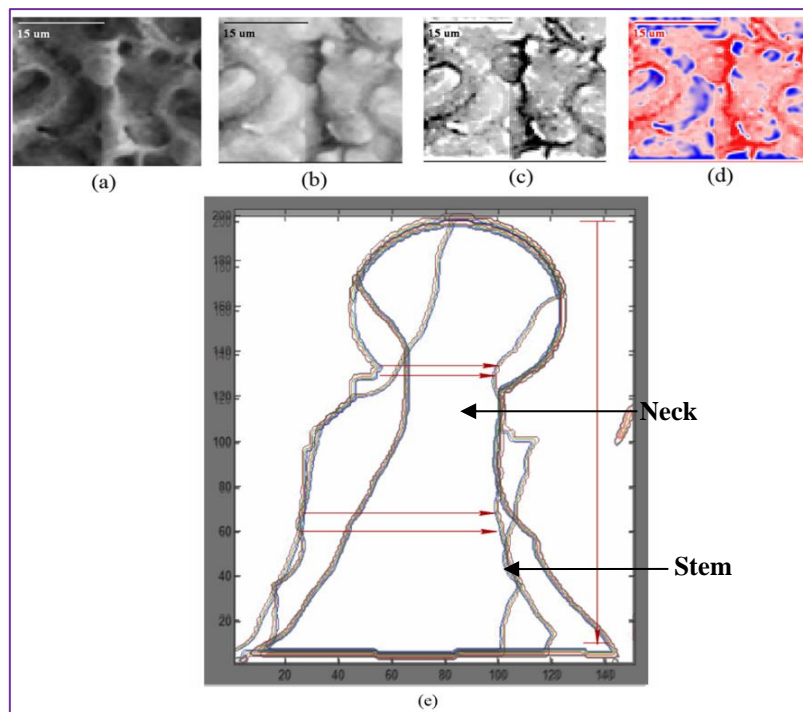
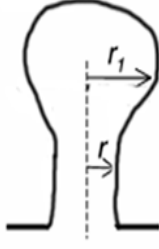


Fig. 3.3: Steps of contour mapping using MATLAB: (a) image acquisition, (b) inverting the image, (c) sharpening the outlines, (d) feature detection, (e) overlaying and dimensional measurement

TABLE 1: DATA OBTAINED THROUGH CONTOUR MAPPING

Contact geometry	Pillar radius, r (μm)	Tip dimensions (μm)	E^* (MPa)	Splitting efficiency (at $P_p = 1\text{mN}$) Exp (Theory)
Mushroom tip 	10	$r_t \sim 12.9 \pm 0.3$	$2.50^{(e)}$	-2.26
	25	$r_t \sim 32.1 \pm 1.5$	$1.81^{(e)}$	

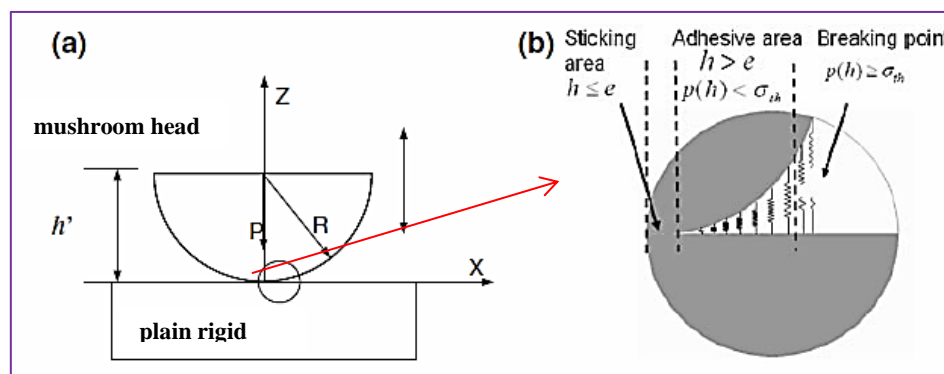
III.D. Numerical Modelling and Post-Processing

The commercial multi-physics and Finite Element Analysis software, COMSOL, was used to do the FEA operations on the model. The aspect ratio and co-ordinate data were loaded in SolidWorks and a 3D- model of an array of mushroom head geometries were generated by directional extrusion.

The sphere above the rigid half-space is assumed to be linearly elastic with Young's modulus E and Poisson's ratio ν . Contact occurs when $h' - R \leq e$ and the resulting contact area radius is denoted as a ; P indicates the normal load of the contact. The varying clearance along the local geometry is denoted as variable h . For the contact geometry in Fig. 3.4(a) and (b), a finite element (FE) adhesive contact model is set up and implemented using COMSOL. As shown in Fig 3.4(c), finite element mesh for the contact pairs was constructed with 4-node free tetrahedral elements because studies have proven this efficient meshing algorithm for arbitrary geometries. The surface of the rigid body is modelled as an infinite rigid plane.

To describe the dynamic contact process (approach and separation of the two surfaces) in detail, general FE simulation flow of the contact process is modified, and the interfacial interactions as described by Eqs. 3 and 4 are incorporated into the contact cells. Equation 2 is incorporated into the contact cells. As shown in Fig. 3.4.(b), at the critical moment of the breakage of a pair contact cells (pull-off point), the critical local stress is defined as a tensile stress equal to a theoretical strength of adhesion, i.e., $p(h)$ at r^{th} .

To reveal the geometry details of the contact area, the contact area is divided into two zones namely, the 'sticking area' and the 'adhesive area' according to the attractive or repulsive nature of the interfacial forces. Sticking area is located on the center of the whole contact area comprising of interacting point pairs with $h \leq e$ in Figure 3.4(b). Adhesive area is the round annular part comprising the point pairs with $h > e$ as well as $p(h) < \sigma^{th}$.



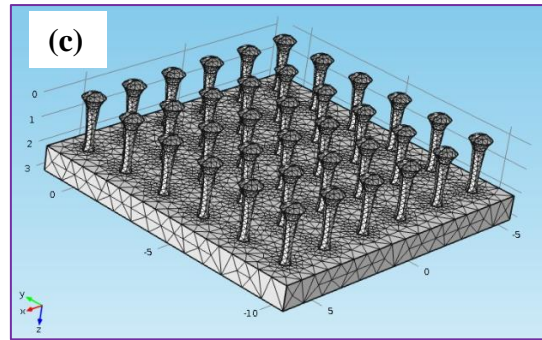


Fig. 3.4: Contact geometry during FE- modeling: (a) The center of the sphere is at a height H' above a rigid half space; (b) Contact occurs when the varying clearance $H = H' - R \leq E$ and the resulting local contact area; (c) FE- modeling of the contact by COMSOL

Clearly, interfacial clearance h is a varying distribution function over the contact area depending on the local deformation and contact geometry. In the modeling, normal load P is defined as the reaction force from the substrate, which equals the vertical force on the substrate in the COMSOL software to keep the contact system in equilibrium.

When $P > 0$ indicates that the contact point pair experiences a repulsive force, while $P < 0$ indicates an interfacial attractive force. The maximum attractive force during detaching process is defined as the pull-off force. To compare with the conventional contact models, we normalize the load P and the deformation displacement “ d ” using interfacial adhesion force $\pi\Delta\gamma R$ as in the following equations:

$$\bar{P} = \frac{P}{\pi\Delta\gamma R} \quad (5)$$

$$\bar{\delta} = \delta \left(\frac{16E^2}{9\pi^2\Delta\gamma^2 R} \right)^{\frac{1}{3}} \quad (6)$$

Where, $\Delta\gamma$ is the work of adhesion, E is the equivalent elastic modulus, and R is the equivalent radius in Hertz contact.

IV. RESULTS AND DISCUSSION

IV.A. Verification of the Model

The elastic adhesive contact of a nano-scale sphere with a smooth semi-finite rigid body is analyzed using the FE adhesive contact modelling module and compared with the results from the conventional adhesive contact models. The sphere is considered with radius $R = 10 \mu\text{m}$, Young's modulus $E = 100 \text{ GPa}$, and Poisson's ratio $\nu = 0.3$. Frictionless contact is assumed. For *Van Der Waals* interaction, D_c (separation energy) usually ranges between 10 and 50 mJ/m^2 , which is assumed as 10 mJ/m^2 according to Th  ry [21]. The effective equilibrium distance of *van der Waals force* is taken to be $e = 0.23 \text{ nm}$. We also adopted $r^{th} = 20 \text{ MPa}$ according to earlier research by Johnson et al. [17]. At each equilibrium step, the local interfacial stress is shown to be dependent on the varying clearance and deformation according to Eqs.1 and 2. To focus on the adhesion force, the modeling begins from a contact state with pure adhesive force and zero normal loads [Fig. 4.1]. By increasing and then decreasing the interfacial deformation displacement d , the variations of normal load and contact area are calculated based on the equilibrium condition.

Within the separation step when the deformation displacement is gradually decreased, the FE contact cells outside the contact area “detach” when the local tensile stress increases up to the critical stress r^{th} . The contact area is decreased until the whole breakage of the contact objects. Then the deformation curve is obtained and normalized by Eqs. 3 and 4. The force curve of FE modeling falls in the gap between the JKR model and DMT model due to the adopted interfacial force model in Eqs.1 and 2. Further verification can be ensured by observing the trend of the displacement generated in the FE -interface and comparison with the actual case observed in the works of Chan et al. [13].

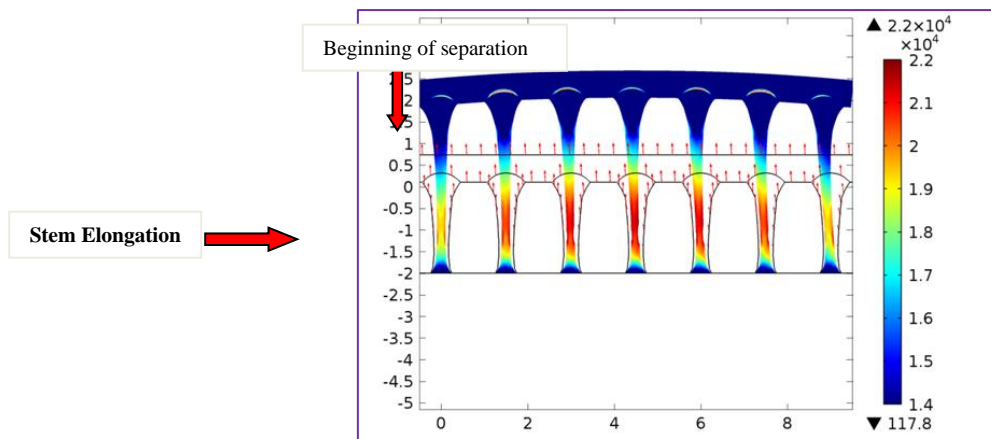


Fig. 4.1: Deformation displacement contour during approach and separation. The beginning of contact separation and then stem elongation are precursors to the final failure.

The plot shown in Fig. 4.2 further confirms with the prediction in the work by Li and Chang [10], which mentions that the separation will start from the perimeter in contact with the adhesion block. The example of mechanism by Chan et al. [13] only considers energy dissipation at the interface, but the three-dimensional (3D) geometry of a patterned interface also plays an important role.

The aspect ratio of the features increases conformability to the contacting surface. Higher-aspect ratio features are more compliant, which improves their adaptability to rough surfaces and maintains interfacial contact. This mechanism cannot be overemphasized, as adhesion is most dependent upon the ability of two surfaces to establish contact.

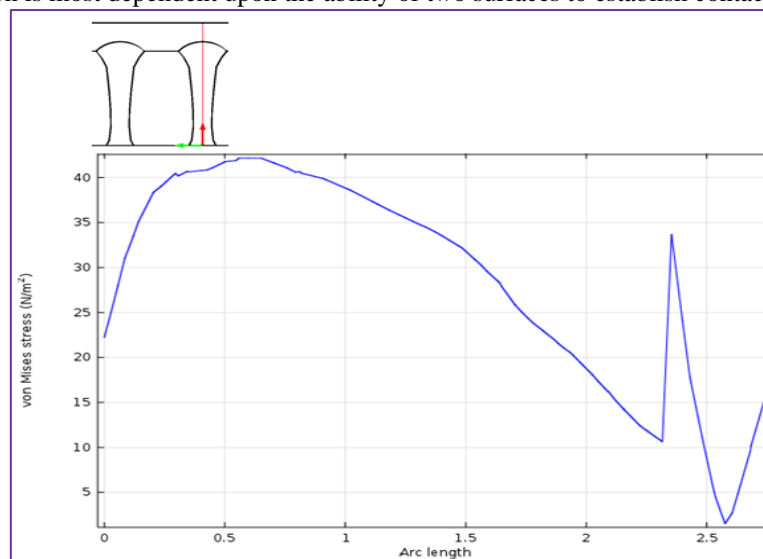


Fig. 4.2: Spike in von Mises stress values around the contact perimeter of the mushroom-head where the separation occurs

Additionally the aspect ratio of the fibrils structures defines the constraints at the interfaces. Less constraint leads to a decrease in the stress concentration along the interface. In other words, increasing the aspect ratio of the feature effectively “blunts” an interfacial crack during separation. This in turn, reduced the probability of a sudden, abrupt, and unforeseen fracture failure through the coating structure. Thus, conclusions can be drawn that geometric shape features is what influences the failure behavior of the micro fibrils.

Further validation study was carried out by ensuring “mesh independence” for the proposed model. The mesh refinement analysis yielded the following result where it can be seen that after 2x refinement [Fig. 4.3], the relative errors didn’t exceed beyond a factor of 10^{-4} . This proved the mesh independence of the model and solving method adopted. So a two level refined mesh approach was adopted for the rest of the simulation.

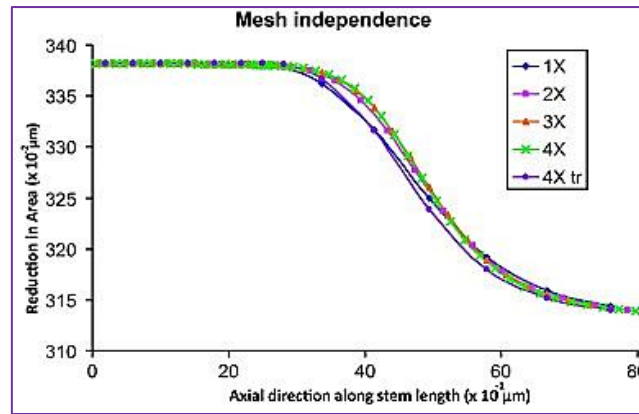


Fig. 4.3: Mesh independence study on one of the parameters of interest (reduction in area along stem length)

The 2x refinement ensured that the simulation runs could be managed within a feasible time-scale while maintaining an appreciable level of accuracy in the output data. The limitations to the high-aspect ratio feature are the tendency for nearest neighbors to collapse because of inter-feature attractive forces, and the ultimate fracture force of the fibrils decreases as the spheroid diameter decreases.

IV.B. Geometry- based Pull-Off Forces and Increase in Adhesion

In previous experiments, mushroom-shaped fibrils were often fabricated with a peeling angle $\theta=90^\circ$ to study the adhesion behaviors and to compare the adhesion force with that of other contact shapes [2]. Theoretical models for the adhesion of a mushroom-shaped fibril with $\theta=90^\circ$ were established to explain the experimental observations.

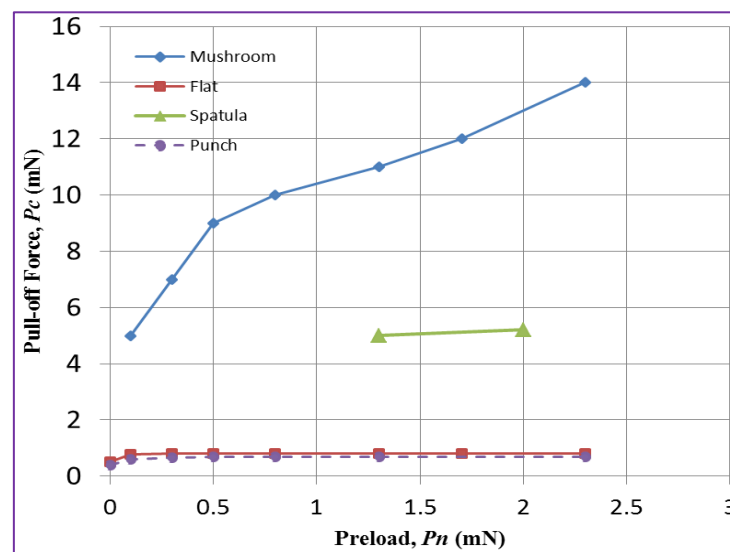


Fig. 4.4: Adhesion force comparison of the four different geometry-tips vs. pre-applied load.

The geometrical effects with various parameters of the mushroom shaped fibril on the adhesion force were systematically investigated in this research to explore the superior adhesion mechanism of such a structure. The substrate is assumed a rigid hemisphere with uniform radius of 10 nm. The four tip-shapes are selected as flat punch, spatula tip, mushroom, and sphere; and the results are shown in Fig. 4.4.

As shown in Fig. 4.4, the model runs with the mushroom-head geometry showed a significant increase in adhesion energy with increase in preload. Based on Fig. 4.4, the pull-off force for mushroom head is > 3 mN, higher than for the spatula. Other observations that can be made are:

- (i) The pull-off force increases sharply as the pre-applied load increases at a low load range, but approaches a stable value. When the preload is large enough, the pull-off forces are almost independent on the pre-load.
- (ii) Different contact geometries result in different pull-off force peaks.

The pull-off force of the mushroom-head shape increases sharply compared with the other geometries studies. After a proper pre-load, the mushroom shape owns a maximum pull-off force, followed by spatula tip, flat and punches shapes, respectively. The test runs for the spatula head were significantly more time consuming, and that is why only limited test runs were performed.

V. CONCLUSIONS

Adhesion is an imperative catalyst in the durability of thermal-barrier-coatings and mechanical adhesion mechanisms, which can provide a strong, uplift in the protection of TBC's from the spallation and de-bonding failures. The numerical modeling method was proposed by drawing an analogy between biologically adhesive, fibrillar, 'mushroom-head' geometries and the spheroidal micro-features on an EPP-treated surface. A method to quantify the adhesion strength numerically from this modeling was also proposed.

Due to the lack of a physical method to measure the profiles on the EPP-treated surfaces, a method based on optical contour recognition was adopted. The cell-tracer algorithm was used to model the unique geometry observed in EPP-treated surfaces. The generated geometry was then used to run adhesion energy tests on a software based OSE (Operational Simulation Environment).

From the simulation results, it can be deduced that the unique geometry generated by EP-process was indeed beneficial for adhesion mechanism. The improvement in pull-off-force in case of 'mushroom-heads' as compared to other patterns was almost 10- folds. As the congruity of the aspect ratio of these mushroom heads can be maintained, the adhesion improvement should persist. There is a striking semblance between the JKR theory of 'dry van der Waals adhesion' in close proximity of micro/nano structures, and the geometrically complex structures evolved by Gecko like animals. However that this research was able to approximate the function of the setae tip, and tie it to a process of artificial synthesis, which determined the empowering factors behind enhanced adhesion.

In conclusion, the findings of this study can be attributed to the following broader general comments:

- (i). EPP- treatment effectively modifies the surface of metals and alloys to be coated and produces an expedient morphological change that increases adhesion.
- (ii). The EPP- surface features have a longer shelf life than many of its comparable technologies, making it even more economically lucrative.
- (iii). The "mushroom-head" geometry has been classically proven to be an excellent choice for bio-adhesion, and this work further strengthens that argument, and encourages the new research in this direction.

ACKNOWLEDGEMENTS

The authors gratefully acknowledge the support received from the USA's NASA-EPSCoR program (NASA/LEQSF (2009-12) Phase 3-03, LSU Account Nos: 127-85-4117 & 127-85-4118) without which, this work would not have been possible.

REFERENCES

- [1] Cho, Y.S., Han, H., and Kim, W.D., "Numerical Analysis of the Adhesive Forces in Nano-Scale Structure", *Journal of Bionic Engineering*; vol.3: pp.209-16., 2006.
- [2] Yan, Y.Y., "Recent Advances in Computational Simulation of Macro-, Meso, and Micro Scale Biomimetics Related Fluid Flow Problems", *Journal of Bionic Engineering*; vol.4: pp.97-107., 2007.
- [3] Liang, J., Wahab, M.A., and Guo, S.M., "Surface Cleaning and Surface Modifications through the Development of a Novel Technology of Electrolytic Plasma Process (EPP)", *World Journal of Engineering*, Vol. 7(3), pp. 54-61, 2010.
- [4] Autumn, K., Sitti, M., Liang, Y. A., Peattie, A.M., Hansen, W.R., and Sponberg, S., "Evidence for van der Waals adhesion in gecko setae". *Proceedings of the National Academy of Sciences of the United States of America* 2002;99:12252-6.
- [5] Dai, Z., Sun, Jr. A., "Biomimetic Study of Discontinuous-Constraint Metamorphic Mechanism for Gecko-Like Robot". *Journal of Bionic Engineering* 2007;4:91-5.
- [6] Ji, A., Han, L., and Dai, Z., "Adhesive Contact in Animal: Morphology, Mechanism and Bio-Inspired Application". *Journal of Bionic Engineering* 2011; 8:345-56.
- [7] Liang, J., Hossain, N. I., Wahab, M.A., and Guo, S.M., "Improvement of Corrosion Resistance on a Low Carbon Steel 1018 in 3.5% NaCl Solution by Electrolytic-Plasma-Process (EPP)." *ASME 2012 International Mechanical Engineering Congress & Exposition 2012*, Houston, Texas, USA (2012): 145-60
- [8] Liang, J., A Study on the Cleaning and Modification of Metal Surfaces by Direct Current Cathodic Electrolytic Plasma Process, Ph.D. Dissertations, Louisiana State University and A. & M. College, Baton Rouge, LA 70803, USA. 2013.
- [9] Gupta, P., Tenhundfeld, G., Daigle, E.O., and Ryabkov, D., "Electrolytic plasma technology: Science and engineering- An overview". *Surface and Coatings Technology* 2007;201:8746-60.
- [10] Del Campo, A., Geiner, C., and Arzt, E., "Contact Shape Controls Adhesion of Bioinspired Fibrillar Surfaces," *Langmuir*, vol. 23, pp. 10235-10243, 2007.
- [11] Li, G., Chang, T., "Effect of head shape on the adhesion capability of mushroom-like biological adhesive structures," *Acta Mechanica Solida Sinica*, vol. 24, pp. 320-325, 2011.

- [12] Zhang., X., Wen, S., "Finite Element Modeling of the Nano-scale Adhesive Contact and the Geometry-based Pull-off Force". Tribology Letters 2010;41:65-72.
- [13] Chan, E.P., Greiner, C., Arzt, E., and Crosby, A.J., "Designing model systems for enhanced adhesion," MRS Bulletin, vol. 32, pp. 496-503, Jun 2007.
- [14] Dai, Z., Gorb, S., "Contact mechanics of pad of grasshopper (Insecta: ORTHOPTERA) by finite element methods". Chinese Science Bulletin 2009;54:549-55.
- [15] Kim, W.S., Yun, I.H., Lee, J.J., and Jung, H.T., "Evaluation of mechanical interlock effect on adhesion strength of polymer-metal interfaces using micro-patterned surface topography". International Journal of Adhesion and Adhesives 2010;30:408-17.
- [16] Weiss, H., "Adhesion of Advanced Overlay Coatings: Mechanisms and Quantitative Assessment." Surface and Coatings Technology 71.2 (1995): 201-07.
- [17] Johnson, K.L., Kendall, K., and Roberts. A.D., "Surface Energy and the Contact of Elastic Solids." Proceedings of the Royal Society A: Mathematical, Physical and Engineering Sciences 324.1558 (1971): 301-13
- [18] Yao, H., Gao, H., "Optimal shapes for adhesive binding between two elastic bodies". Journal of colloid and interface science 2006; 298:564-72.
- [19] Liang, J., Zhang, P.G., Wang, K.Y., Guo, S.M., Wahab, M.A., "Cleaning of Oxide Layer on Steel Surface by Electrolytic Plasma Process," Materials Science & Technology- 2011 Conference & Exhibition, Columbus, Ohio, Oct., (2011).
- [20] Cionea, C., Microstructural of surface layers during electrolytic plasma processing, Ph.D. Dissertation, University of Texas at Arlington, 2010.
- [21] Meletis, E.I., Wang, F.L., and Jiang, J.C., "Electrolytic plasma processing for cleaning and metal-coating of steel surfaces," Surface and Coatings Technology, pp. 246-256, 2002.
- [22] Hossain, N.I., Numerical evaluation and analysis of the adhesion phenomena in thermal-barrier -coating systems through bio-mimicking plasma process, Master Thesis, Louisiana State University And A. & M. College, Baton Rouge, LA 70803, USA, 2011.
- [23] Wang, Q., CellTracer: Software for Image Segmentation and Lineage Mapping for Single-cell Studies Modeling, Duke University & NSF, June- 2008. Web.